CrossMark

Local commute-time guided MDS for 3D non-rigid object retrieval

Hela Haj Mohamed[1] · Samir Belaid[1] · Wady Naanaa[2] · Lotfi Ben Romdhane[1]

Abstract

In this paper, we propose a 3D non-rigid shape retrieval method based on canonical shape analysis. Our main idea is to transform the problem of non-rigid shape retrieval into a rigid shape retrieval problem via the well-known multidimensional scaling (MDS) approach and random walk on graphs. We first segment the non-rigid shape into local partitions based on its salient features. Then, we calculate a local MDS problem for each partition, where the local commute time distance is used as weighting function in order to preserve local shape details. Finally, we aggregate the set of local MDS problems as a global constrained problem. The constraint is formulated using the biharmonic function between local salient features. In contrast to MDS method, the proposed local MDS is computationally efficient, parameters free and gives isometry-invariant forms with minimum features distortion. Due to these advantageous properties, the proposed method achieved good retrieval accuracy on non-rigid shape benchmark datasets.

Keywords Non-rigid 3D shape deformations · 3D canonical forms · Multidimensional scaling · 3D non-rigid shape retrieval · Intrinsic metrics on 3D shapes · Commute-time distance

1 Introduction

In the last few years, the recognition task of non-rigid 3D objects, has become a significant challenge for modern shape retrieval methods. Many algorithms are proposed to overcome the challenge [1–4]. They are classified mainly into algorithms based on local features, topological structures, isometric-invariant global geometric properties, direct shape matching, or canonical forms. In the last category, the authors of [5–8] proposed to transform each 3D model into a pose-invariant canonical form. This proposal allowed several rigid shape descriptors to perform non-rigid shape retrieval. The use of Multidimensional Scaling Method (MDS) is one of the most used methods for generating 3D canonical forms. However, the main challenge for this method remains the construction of canonical forms with well-preserved features and with a low time-complexity.

This paper introduces a novel method for 3D non-rigid object retrieval based on the MDS approach by considering local shape features. Our main idea is to use the commute-time distance criterion guide the embedding process in the optimization stage. In fact, we use this intrinsic metric to penalize the geodesic distance between two nodes and increase the robustness of the proposed approach. To begin with, we partition the global MDS problem into a set of sub-problems and generate corresponding local 3D canonical forms. More specifically, we are building on feature points extracted from the target model to generate the set of local patches. These patches are spatially related. To compute their associated 3D canonical form, we solve a nonlinear minimization problem. As spatial relationship constraints, the biharmonic distance is a good choice that preserves topological structure of the model in the embedding space. Note that this solution reduces the high computational cost of geodesic distance between each pair of vertices. An evaluation of the quality of the obtained canonical forms has been published in [9], are used two different measurements: the compactness measure and the Haussdorf distance. Then, the resulting 3D objects are used for 3D non-rigid object retrieval using a view-based descriptor.

The rest of the paper is organized as follows: In Section 2, we briefly present MDS-based techniques. In Section 3,

✉ Hela Haj Mohamed
  hajmohamedhela@yahoo.fr

1 MARS Research Lab Higher Institute of Computer Science and Telecom (ISITCom), University of Sousse, Sousse, Tunisia

2 University of Tunis El Manar, Tunis, Tunisia

we establish the mathematical background of the proposed method. In Section 4, we detail our method for generating the 3D canonical form. Finally, we report our experimental results for the retrieval task in Section 5.

2 Canonical shape analysis

The multidimensional scaling is widely considered as an efficient approach in the dimensionality-reduction area [10–12]. The basic idea is to map data, described in initial feature space, into a small-dimensional Euclidean space. The data are embedded in such a way as to preserve, as much as possible, the affinity between each pair of data points.

In the 3D domain, Elad and Kimmel [5] argued the use of the MDS method to embed surface points of 3D non-rigid shapes into a three-dimensional Euclidean space. In this latter context, the dissimilarity is measured by geodesic distances between all pairs of points in the shape. The resulting representation is known as the canonical form for a given 3D mesh. In fact, the authors proved that applying MDS in 3D non-rigid shapes enables the calculation of an isometric invariant representation while undoing its deformations. Therefore, the canonical shape is treated as a rigid shape instead of the non-rigid one, in the retrieval task. This method has two main drawbacks: the high time complexity and the features distortion of the shape.

To accelerate the MDS step, several approaches have been proposed, such as spectral MDS [12] and Nystrom MDS [13]. The cited approaches achieve the goal by searching a low-rank approximation of the affinity matrix. Whereas other methods, e.g. [14] and [15], focused on speeding up the computing of the exact geodesic distances.

To improve the MDS approach, several authors proceed by minimizing the feature shape distortion and enhancing the resultant-canonical form quality. For instance, Lian et al. [6] created a feature preserving canonical form, by considering MDS embedding results as references, and then they naturally deformed the original meshes against them. Nevertheless, this method is sensitive to topological errors, although it is quite robust against mesh segmentation. In addition, the method suffers from a high computational time due to the computation of geodesic distances between all pairs of vertices. To circumvent this difficulty, meshes are reduced so that they contain about 2000 vertices, before applying the MDS embedding procedure. However, this solution can affect the quality of the mesh as well as its local features.

More recent methods avoided using the geodesic distance as an intrinsic metric. Boscaini et al. [8] and Pickup et al. [7] both used only a local distance between adjacent shape vertices. Boscaini et al. [8] proposed to perform the embedding using a physical model of electrostatic repulsion. The method is fast but still distorts the local shape details. Furthermore, Pickup et al. [7] maximized the distance between pairs of detected feature points while preserving the mesh's edge lengths. The proposed method results in less shape distortion, but occasionally fails to completely stretch out the shape limbs. In addition, it is not fully automatic, and requires manual-tuning of many parameters. The authors of [16] proposed to perform the unbending on the skeleton of the mesh and used this to guide the deformation of the mesh itself. They successfully saved computational time, and reduced distortion of local shape details. However, this method is sensitive to topological errors that may corrupt the mesh and it is designed to work on objects which have a natural skeletal structure. Taking a different direction, Rustamov [17] avoided the use of geodesic distances and found a pose invariant representation of the mesh based on the eigen decomposition of the Laplace-Beltrami operator. The Global Point Signatures (GPS) canonical forms are much faster to compute. However, this method severely distorts local shape features.

In this context our idea is to accelerate the computation step of the geodesic matrix by partitioning the mesh surface into a set of local patches whose number is automatically determined for each object. Then, we propose to calculate the approximate geodesic distance between all pairs of points in the same patch. The global affinity matrix is then constructed by combining the set of all local geodesic matrices. In order to model the relationship between them, we impose a metric constraint. Our method differs from those exposed in the above cited works with respect to the preservation of local shape features. We propose to weight the geodesic distance by a commute time metric to guide the embedding. In fact, we rely on the robustness of this metric to improve results and decrease the sensitivity of canonical forms to topological noise.

3 Mathematical background

In this section, we introduce some fundamental concepts used in our method.

3.1 MDS and SMACOF algorithms

The Classical MDS method, proposed by Elad and Kimmel [5] is based on a symmetric distance matrix D_F which is defined by

$$D_F = \begin{bmatrix} d_F^2(Y_1, Y_1) & \dots & d_F^2(Y_1, Y_N) \\ . & \dots & . \\ . & \dots & . \\ . & \dots & . \\ d_F^2(Y_N, Y_1) & \dots & d_F^2(Y_N, Y_N) \end{bmatrix} \tag{1}$$

with $d_F^2(Y_i, Y_j)$ is the geodesic distance between the pair of vertices Y_i and Y_j, computed using the fast marching method [18] in the feature space. The inner product matrix (i.e., the Gram matrix) G_E is calculated in the embedded Euclidean space by

$$G_E = -\frac{1}{2} J D_F J \qquad (2)$$

where

$$J = \frac{1}{N} \mathbf{1}\mathbf{1}^T \qquad (3)$$

where $\mathbf{1}$ denotes the N-one vector. The Euclidean embedding of these distances is then computed using the eigen-decomposition of the Gram matrix G_E. So, the classical MDS minimizes the following energy function:

$$E_{S1}(X) = \| Q(\Lambda - \overline{\Lambda}) Q^T \|^2 \qquad (4)$$

where $\| \bullet \|$ denotes the Frobenius norm of the squared matrix elements, $\Lambda_{m \times m} = \mathrm{diag}(\lambda_1, \lambda_2, ..., \lambda_m)$ with the eigenvalues of G_E ordered so that $\lambda_1 \geq \lambda_2 \geq ...\lambda_k \geq 0$, Q denotes the matrix having as columns the corresponding eigenvectors and m is the dimension of the embedded Euclidean space. For a given point Y_i on the mesh, its MDS embedding X_i is calculated as

$$X_i = (\lambda_1^{\frac{1}{2}} Q_1(Y_i), \lambda_2^{\frac{1}{2}} Q_2(Y_i), \lambda_3^{\frac{1}{2}} Q_3(Y_i)) \qquad (5)$$

where λ_1, λ_2 and λ_3 are respectively the first three eigenvectors and corresponding eigenvalues of G_E.

The authors of [5] improved their results by suggesting a standard optimization algorithm. The Least Squares technique uses the SMACOF (Scaling by Maximizing a Convex Function) algorithm [10] to minimize the following stress function $E_S(X)$:

$$E_S(X) = \Sigma_{i=1}^N \Sigma_{j=i+1}^N \omega_{i,j} (d_F(Y_i, Y_j) - d_E(X_i, X_j))^2 \quad (6)$$

where N is the number of vertices, the $w_{i,j}$'s are weighting coefficients, $d_F(Y_i, Y_j)$ is the geodesic distance between vertices Y_i and Y_j in the original mesh, and $d_E(X_i, X_j)$ is the Euclidean distance between vertices X_i and X_j of the resulting canonical mesh X. The algorithm iterates until $|E_S(X_i) - E_S(X_{i+1})|$ is less than a user-defined threshold. The overall complexity of the MDS algorithm is $\mathcal{O}(N^2 \times \texttt{NumOfIterations})$.

In this paper, we adopt the Least Squares technique and the SMACOF algorithm to compute the 3D canonical form.

3.2 Intrinsic distances on 3D mesh

Several approaches were proposed to compute intrinsic distances on 3D mesh. These approaches can be categorized as primal or dual. For example, computing exact or approximate geodesic distance is a primal approach because it operates directly on the mesh surface. As geodesics have

a number of drawbacks (sensitive to noise and topology and not globally shape-aware), dual distances overcome these problems.

Spectral distances are the most popular dual distances. They are based on relationships between a set of real-function values for inferring distances. As examples of distances, we cite the diffusion [19], commute time [20], and biharmonic [21] distances. Unlike the geodesic distance, the diffusion distance is related to heat diffusion on the shape. It captures the average number of paths between two points, in a fixed time, rather than a single path.

The diffusion distance is calculated based on the Laplace-Beltrami operator and the heat equation, which is defined as follows

$$(\Delta_X - \frac{\partial}{\partial t}) u = 0. \qquad (7)$$

The solution of (7) is called the heat kernel $h_t(x, y)$. It provides the heat value at time t at point $y \in X$ starting from $x \in X$. The values of $h_t(x, y)$ can be interpreted as the probability of reaching point y by means of a random walk on X having length t and starting from point x. For compact manifolds, the heat kernel can be calculated by means of the eigenfunctions of the Laplace Beltrami operator [22] as

$$h_t(x, y) = \Sigma_{i=0}^k e^{-\lambda_i t} \phi_i(x)\phi_i(y), \qquad (8)$$

where

$$\Delta_X \phi_i = \lambda_i \phi_i. \qquad (9)$$

So, the diffusion distance is defined as

$$d_{X,t}^2(x, y) = \| h_t(x, .) - h_t(., y) \|_{L_2(X)}^2, \qquad (10)$$

and it can also be expressed as,

$$d_{X,t}^2(x, y) = \Sigma_{i=1}^\infty e^{-2\lambda_i t} (\phi_i(x) - \phi_i(y))^2. \qquad (11)$$

where the time parameter t is considered as a scale value. This means that the variance of this parameter controls the qualities of the features around a point x to all the other points. As shown in Fig. 1, at small scales the diffusion distance decreases fastly to reach zero, and highly local shape features are observed from the point of view of the red point. While for large values of t, the distance decreases slowly to capture the global structure of the shape. The setting of parameter t introduces the problem of scale selection. To solve this problem, the diffusion distance is integrated over all times. The new distance is called the commute time distance, and is given by

$$dc_X^2(x, y) = 2 \int_0^\infty d_{X,t}^2(x, y) dt \qquad (12)$$

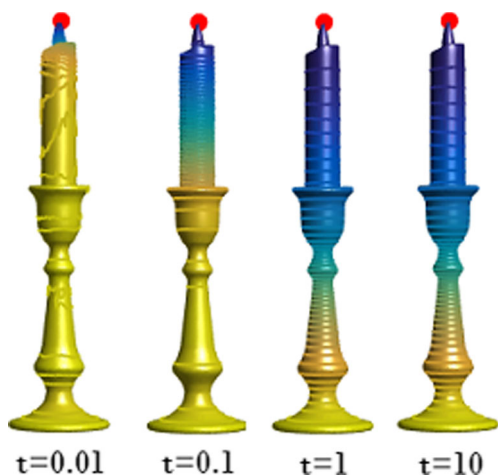$$= \Sigma_{i=1}^\infty \frac{1}{\lambda_i} [\phi_i(x) - \phi_i(y)]^2. \qquad (13)$$

Fig. 1 Example of a mesh surface colored according to the diffusion distance starting from the red point. The color scale indicates different t value

This distance reflects the average number of all possible paths connecting two points, contrary to the diffusion distance that considers only paths of length t. Thereby, the more paths connect x with y, the smaller is their commute time distance. In addition, the commute time captures the connectivity structure of the graph volume which makes it more robust to structural disturbance and topological changes unlike geodesic distance [23]. These advantages motivate our choice to use the commute time distance values in the MDS problem as a weighting function in the stress equation (6). Our idea is motivated by the fact that vertices on the same class have the same value of the commute time distance. This weighting will be preserved as much as possible in the embedding space in order to have the same features as in the original space. In fact, we aim to overcome the drawbacks of the geodesic distance, to ameliorate the resulting canonical form and to preserve its features.

The biharmonic distance is another distance based on the common "cotangent formula" discretization of the Laplace-Beltrami differential operator on meshes. It was proposed

by Lipman et al. in [21] and its discrete version is defined as follows

$$dB(x, y)^2 = \Sigma_{i=1} \frac{(\phi_i(x) - \phi_i(y))^2}{\lambda_i^2}. \tag{14}$$

The latter distance is based on the biharmonic differential operator, nevertheless, it applies different (inverse squared) weighting to the eigenvalues of the Laplace-Beltrami operator. Figure 2 shows examples of geodesic distances, commute-time distances and biharmonic distances on mesh. As we clearly see, the shape of isolines reflects the intrinsic properties of each function. Regarding the geodesic distance, the isocontours far from the source depend on the exact placement of the starting point. This means that the distance is not shape-aware. While the isolines of the commute time distance are not equally distributed and very close to the source point. The shape of the biharmonic distance provides a trade-off between a nearly geodesic behavior for small distances and global shape-awareness for large distances. In addition, its isocontours are evenly spaced on the whole mesh surface.

Generally, each distance has its own characteristics as an intrinsic metric. In this paper, we benefit from all these properties in order to properly describe the 3D mesh surface and preserve its local features in the embedding space as much as possible. The details of the proposed method are described in the next section.

4 Local features-based 3D canonical form

The main idea behind our method is to construct 3D canonical forms that are invariant to the shape pose. The resulting form is then usefully treated as a rigid shape instead of the non rigid one involved in the retrieval task. Figure 3 shows examples of 3D canonical forms produced by our method. It is easy to see that the MDS embedding naturally deformed the original shapes by stretching out as
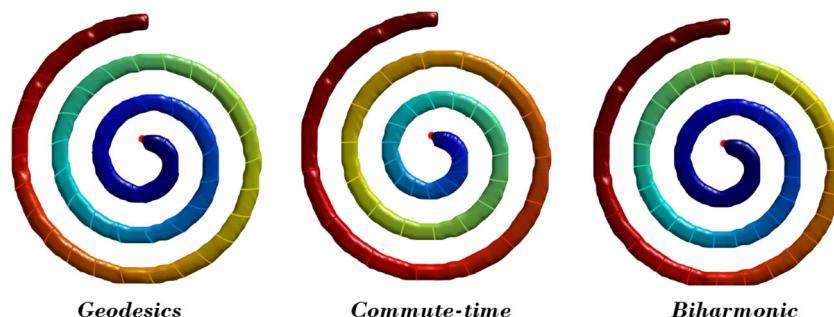

Fig. 2 Analysis on 3D shape intrinsic distance metrics. The geodesics are computed using the fast marching algorithm starting from the red point. All the shapes are color-coded according to the distances:

geodesic distance, commute-time distance and biharmonic distance. Blue indicates small distance and red indicates long one

Fig. 3 3D canonical forms for a selection of the SHREC'15 dataset produced by our method.
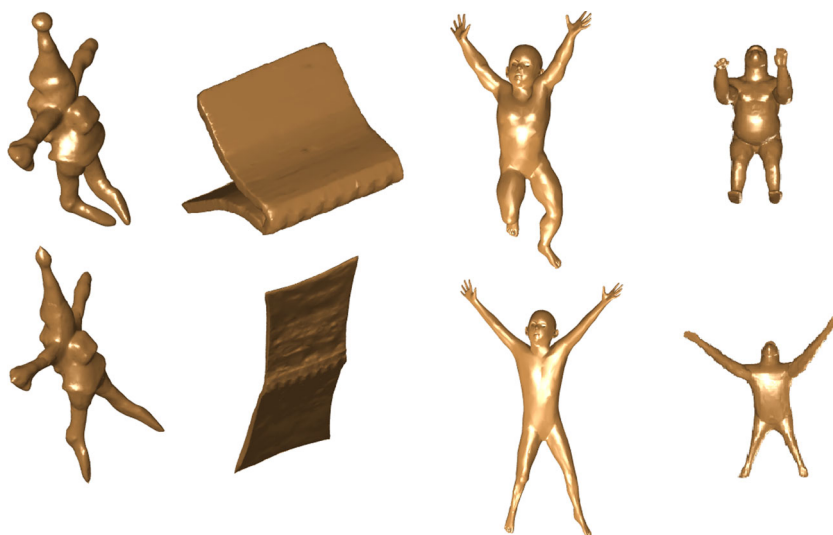
much as possible its limbs. For this reason, we resort to calculating the canonical form in a local way. We start by detecting the limbs of a given model using an automatic and unsupervised 3D salient point detector. We use the local maximum of the Auto Diffusion Function (ADF) [24] defined on the mesh surface as:

$$ADF_t = K(x, x, \frac{t}{\lambda_1}) = \Sigma_{i=0} e^{-t \frac{\lambda_i}{\lambda_1}} \phi_i^2(x) \qquad (15)$$

where λ and ϕ are eigenfunctions of the Laplace-Beltrami operator (LBO). This scalar function is controlled by a single parameter t which can be interpreted as a feature scale. The natural feature points of the shape are the set of local maximum of the ADF located on the extremities of deformable patches. A proof of the invariance of extracted points to non-rigid transformation, scaling, occultation and their insensitive to noise is given in [1].

The set of detected feature points are considered as seeds to partition the 3D mesh into local regions using the Voronoi diagram. Each local patch is then described by an affinity matrix Δ, whose component $\delta_{i,j}$ is equal to the length of the shortest path connecting vertex i to the vertex j. This idea aims to minimizing the computation cost of the geodesic distance and avoids exploring all the paths between every pair of points in the original space. Thus, the estimated complexity of this algorithm is $\mathcal{O}(km_k^2)$, where k denotes the number of local patches and m_k is the size of the kth region. In order to speed up the computation of geodesic distances, we used the heat method proposed by Crane et al. in [25], which gives an approximation of the geodesic distance by exploiting heat kernels. As shown in Fig. 4, Geodesics in heat is almost the same with exact geodesics. Nevertheless, this approximation gives similar results of the embedding

form with high convergence speed. Figure 5 illustrates the comparison of canonical forms, while dissimilarity is computed using Fast marching algorithm and heat geodesic method. We use the Matlab source code available on the web site of Bronstein et al. book's [26] to calculate the canonical form.

To preserve local features of the mesh, we do not consider all pairs of features in the same manner. However, we enforce a target weight between all connected vertices i and j in the same region. The value of $w_{i,j}$ is set according to the value of the commute-time distance $c_{i,j}$. Notes that this is the expected time taken by the random walk to travel from i to j in both directions. Therefore, if $c_{i,j}$ is small, then $\delta_{i,j}$ should also be small enough to minimize the stress function given in (6).

As a next step, we aim to assemble local affinity matrices and create final canonical form of a given model. To do this, a constraint between different partitions is needed. This constraint is formulated as a spatial relationship associating the feature points set to local patches. Thus, we made the choice of the biharmonic distance [21] given in (14).
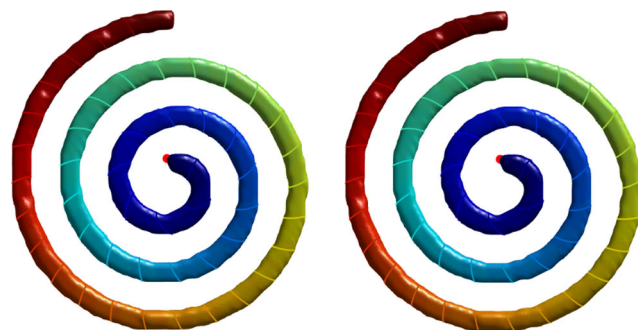

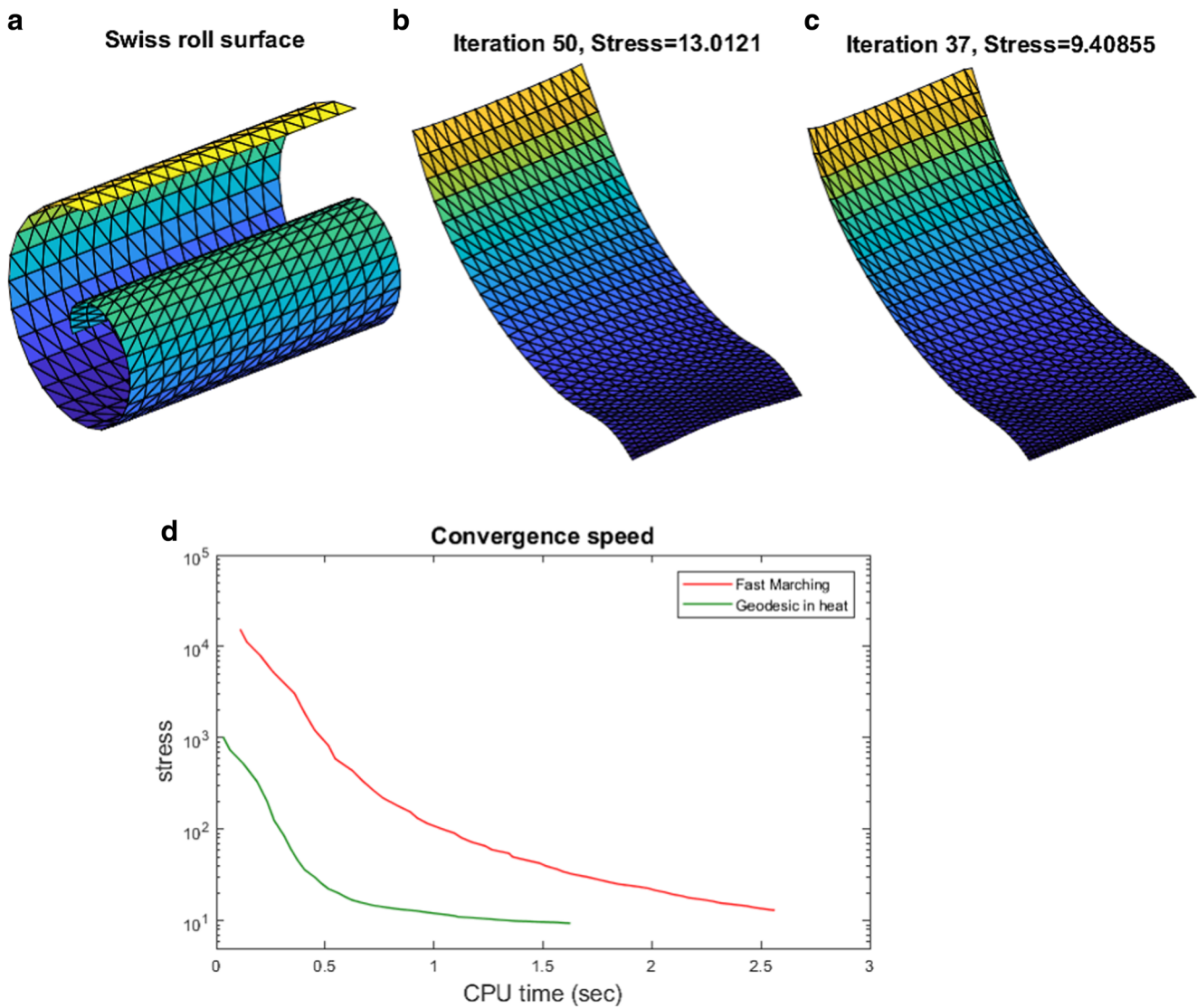**Fig. 4** Left: the exact geodesics. Right: the geodesic in heat

Fig. 5 Swiss Roll surface (**a**) and its 3D canonical form using the classical MDS, **b** geodesic distance is computed by the fast marching algorithm and heat geodesic method (**c**). Their convergence speed is plotted in (**d**)
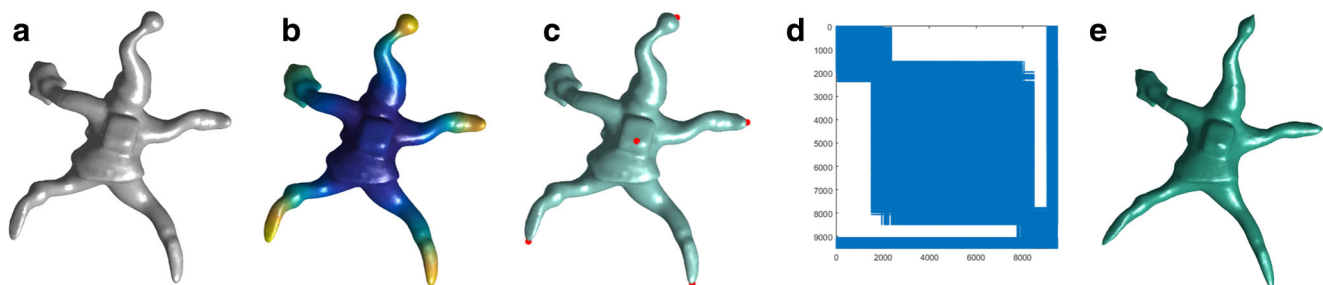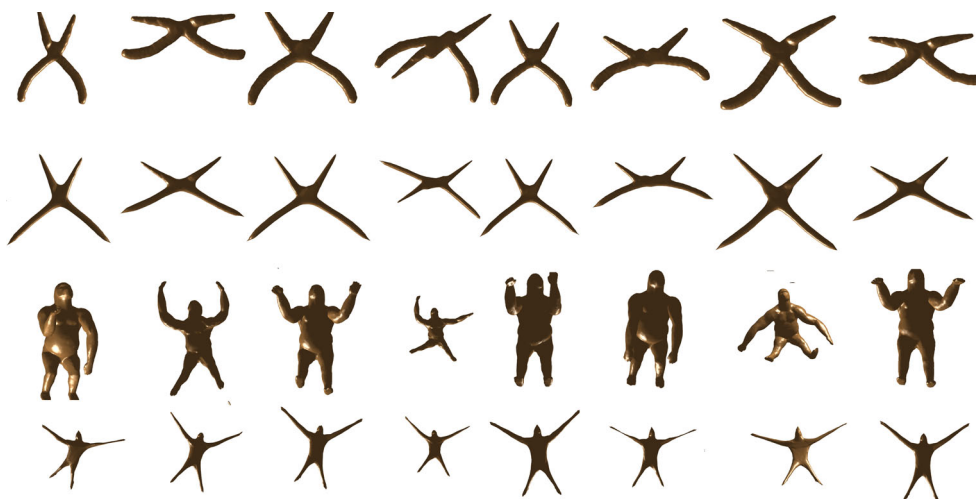

Fig. 6 Mainly steps of our procedure that employs the local features (**c**) extracted by the ADF scalar function defined on the mesh surface (**b**) to generate final 3D canonical form of the original model (**a**)

Fig. 7 Examples of canonical forms of each mesh

Roughly speaking, we reformulated the final stress function to be minimized as:

$$S(X) = \Sigma_k \Sigma_{i,j \in P_k} \frac{c_{i,j}^2}{\delta_{i,j}^2}(\delta_{ij} - d_{i,j})^2$$
$$+ \frac{1}{2}\Sigma_{i,j \in F}(ADF_i + ADF_j)(dB_{i,j} - d_{i,j})^2 \quad (16)$$

where k is the number of local patches, F is the set of feature points, $\delta_{i,j}$ is the local geodesic distances in each region P and $dB_{i,j}$ is the biharmonic distance between feature points.

Figure 6 shows an overview of the performance of our method to compute the canonical form (Fig. 6e) on a given 3D object depicted in Fig. 6a. The scalar function ADF is used as an unsupervised detector of feature points (Fig. 6b and c). Figure 6c, represents the overall dissimilarity matrix computed from the set of local patches. For $n = 9501$ vertex, only 17 million values are used to calculate the final canonical form (Fig. 6e).

Several canonical forms of two objects with non-rigid deformations are shown in Fig. 7. Our method successfully produced canonical forms of each shape and eliminates the non-rigid deformations by stretching out the extremities. The obtained results aim to standardize its pose.

4.1 Computational complexity

The computational complexity of the 3D canonical form methods depend on the time complexity of the distance calculation (matrices δ and dB in (16)) and the SMACOF algorithm (see Section 3.1). Geodesic-based methods calculate the geodesic distance between all pairs of vertices using the fast marching algorithm which has a time complexity of $O(N^2 \log N)$, where N is the total number of mesh vertices. Our method calculates geodesic distances between points located in the same local patch only, rather than all pairs. For a local patch on n vertices in average,

with $n \ll N$, the time complexity is $O(n^2 \log n)$. So, the total computational complexity of distance matrices has $O(mn^2 \log n)$, where m is the number of local patches. Note that m is very small compared to N, (for instance, we have $m = 5$ and $N = 60000$, for the human body shape). Moreover, the SMACOF algorithm has a computational complexity of $O(N^2)$, when the distance between all pairs of points is used. Our Algorithm lowers this complexity to $O(mn^2)$.

5 Experiments for 3D non rigid object retrieval

5.1 Run-time

In order to highlight our contribution, we present a run-time comparison between our local method and the global variant based on geodesic distances matrix. We performed run-time tests on a PC with a 2.6 GHz Intel Core i7-4510U CPU and 16 GB of memory. Table 1 shows the timings for computing canonical form of a given mesh with 9500 vertices. Our method takes significantly less time to calculate the dissimilarity matrix compared to the global geodesic distances matrix. The time taken to produce canonical forms using the Smacof algorithm are also reduced using the local geodesic distances. Furthermore, we simplified the original mesh to approximately 2000 vertices before computing the canonical forms. As a result, the run-time is extremely reduced by both methods. This shows that our method depends on the mesh resolution, but it could be run on the original mesh in a reasonable time. In addition, we test the dependence of our method on the number of local features. To do this, we have chosen a simplified model which uses approximately 2000 vertices. Then, we randomly selected a number of feature

points from the mesh surface. These points are uniformly distributed using Lloyd's algorithm [27]. Figure 8 presents a graph showing the time taken to compute associated canonical forms versus the number of features. The run-time remains stable when computing canonical forms with global geodesic distances while it is higher than our method. The run-time taken by our method decreases as the number of features increases. These results are already theoretically predicted in Section 4.1.

5.2 Non-rigid 3D object retrieval

In this section, we present the results of our experiments for 3D non-rigid object retrieval. We used three public databases containing similar models with different types of non-rigid transformations. For each database, we created a new 3D rigid shape database, by transforming each object to its associated canonical form using the proposed method. Then, we used the shape retrieval method of Lian et al. [28] to evaluate the performance of our method for 3D object retrieval. The main principle of Lian method is to calculate the shape descriptor of an object using the bag of features approach and a set of SIFT features. This set is extracted from the 66 different depth images of each object in the dataset. Algorithm 1 describes the main steps of our 3D object retrieval method based on 3D canonical forms.

Algorithm 1 Dissimilarity matrix calculation for 3D object retrieval

---

Input: T: dataset of 3D non rigid object, n: size of T
Output: D: matrix of all pairwise distances between all objects
foreach *3D object $O_i \in T$* **do**
    Compute the associate canonical form of O_i as described in Section 4: ;
    $F_i \leftarrow$ Compute the set of features points from O_i ;
    $P_{ik} \leftarrow$ Compute the local patch for each $f_{ik} \in F_i$;
    $D_{ik} \leftarrow$ Compute the matrix of squared geodesic distances between every two points in P_{ik} ;
    $W_i \leftarrow$ Compute the weight matrix based on commute-time distance and biharmonic distance ;
    $C_i \leftarrow$ Compute the final canonical form using (16);
    $d_i \leftarrow$ Compute the associate descriptor of C_i using Lian's method [28]
end
for $i \leftarrow 1$ *to* n **do**
    for $j \leftarrow 1$ *to* n **do**
        $D_{i,j} \leftarrow L_1(d_i, d_j)$
    end
end
return D;

Table 1 A run-time comparison between our method and the least squared MDS method

	Least Squares MDS		Our method	
	Geodesic	Smacof	Geodesic	Smacof
Original mesh	98.30 min	13.63 min	46.27 min	27.04 s
Simplified mesh	1.68 min	20.75 s	52.60 s	1.75 s

The times taken by our method to produce canonical form is significantly reduced using the original and simplified mesh

The proposed approach was tested on the following benchmarks:

– The database for the McGill 3D Shape Benchmark (MSB) [29]. It contains 255 objects divided into ten classes (Ant, Crabs, Hands, Humans, Octopuses, Pliers, Snakes, spectacles, Spiders and Teddy); the intraclass variations consist in non-rigid transforms applied to the models.

– The database of the SHREC'11 Track (Shape Retrieval on Non-rigid 3D Watertight Meshes) [30]. It comprises 600 watertight meshes with an average of 9300 vertices. The database is evenly divided into 30 classes based on their semantic meanings.

– SHREC'15 Track [2] is a new benchmark for testing algorithms at creating canonical forms for use in non-rigid 3D shape retrieval. The dataset contains models from both the SHREC'11 non-rigid benchmark [30] and the SHREC'14 non-rigid humans benchmark [31]. The total number of meshes in the dataset is 100 meshes, split into 10 different shape classes. Each shape class contains a mesh in 10 different non-rigid poses.

– SHREC'15 non-rigid benchmark [32] contains 1200 meshes with an average 9607 vertices per mesh. The dataset is split into 50 classes, each class contains topological errors.

The following performance metrics were used to evaluate the efficiency of the method results and to compare it with other works were:

– Nearest Neighboor (NN): The percentage of the cases for which the first closest match belongs to the query's class.

– First Tier (FT): The percentage of the models for the $(C − 1)$ closest matches, where C is the cardinality of the query's class.

– The Second Tier (ST): The percentage of the models for the $2 * (C − 1)$ closest matches.

– Discounted Cumulative Gain (DCG): Evaluates the quality of the retrieval list by incorporating the entire list. Since a user is most interested in the first results,
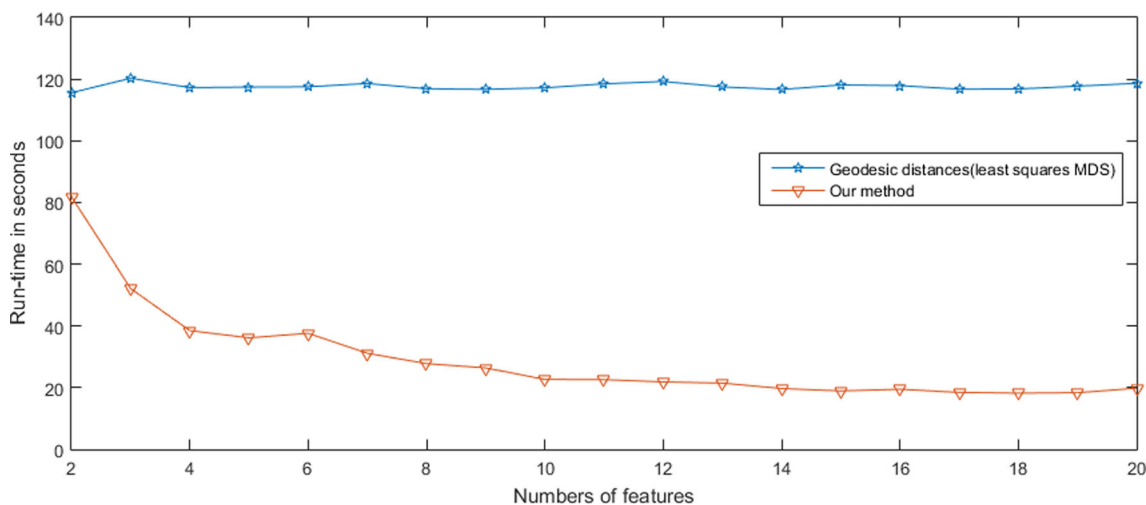
Fig. 8 The run-times in seconds for a different number of features selected from the same mesh surface

correct results near the front of the retrieval list are weighted more heavily than correct results near the end.

– E-measure combines precision and recall metrics into a single number. It is defined as $E = 2 \times (\frac{1}{P} + \frac{1}{R})^{-1}$, where P and R are the precision and recall for a fixed number of retrieved models.

Tables 2 and 3 show a comparison of our method with the highest performing results submitted to the SHREC'11 non-rigid track and MCGill database. The selected methods are all based on canonical forms and use the view-based retrieval method of Lian et al. [28] for non-rigid 3D shape retrieval. Our method achieves the best NN measure for the SHREC'11 non-rigid track and a very competitive performance behind Pickup method [7] and geodesic based methods. Note that our method is fully automatic and does not require all pairs of geodesic distances to be computed. Despite these results, it is clear that the difference between retrieval scores of original meshes and canonical forms is negligible. This is justified by the large difference among classes.

Table 4 shows the retrieval performance on the SHREC'15 canonical forms benchmark [2]. Compared to

geodesic based methods (the Least Squares MDS, non-metric MDS, Fast MDS...), our method achieved a very competitive performance according to all performance measures. Although our method does not use all geodesic distances, the commute time distance guided the embedding to achieve the same performance. This highlights the importance of using spectral metrics to preserve local features of the canonical form.

We also tested the performance of the proposed method on SHREC'15 non-rigid shape retrieval benchmark [32]. The retrieval results are shown in Table 5. Despite the huge size of this dataset and the presence of topological errors within some of the meshes, we achieve good retrieval performance behind the least squares non-metric MDS. It outperforms the GPS method and the Euclidean based method [7]. Our method is also competitive with the skeleton based method although it is sensitive to topological errors. This may be due to the use of the view-based method in the retrieval task. Moreover, and as shown in the precision–recall plots reported in Fig. 9, our method is among the top three best methods.

Table 2 Retrieval statistics for the SHREC'2011 database

Method	NN	1-Tier	2-Tier	e-Measure	DCG
Originalmeshes	0.985	0.746	0.863	0.627	0.931
Classic MDS	0.987	0.855	0.943	0.691	0.964
Fast MDS	0.978	0.795	0.905	0.657	0.945
Least Squares MDS	0.995	0.913	0.969	0.717	0.982
Euclidean based canonical [7]	0.982	0.867	0.964	0.708	0.974
Our method	0.996	0.875	0.956	0.702	0.971

Table 3 Retrieval results for the MCGillBall database

Method	NN	1-Tier	2-Tier	e-Measure	DCG
Original meshes	0.980	0.744	0.896	0.691	0.940
Classic MDS	0.961	0.728	0.868	0.678	0.931
Fast MDS	0.918	0.692	0.860	0.649	0.909
Least Squares MDS	0.996	0.830	0.947	0.778	0.970
Euclidean based canonical [7]	0.969	0.761	0.891	0.710	0.940
Our method	0.972	0.788	0.904	0.736	0.949

Table 4 Retrieval results for the SHREC'15 canonical forms benchmark [2]

	NN	1-Tier	2-Tier	DCG
Original Meshes	0.50	0.567	0.702	0.753
Classic MDS	0.73	0.597	0.741	0.796
Fast MDS	0.66	0.590	0.718	0.789
Least Squares MDS	0.75	0.694	0.829	0.838
Non-Metric MDS	0.77	0.687	0.811	0.836
GPS	0.72	0.556	0.697	0.783
Euclidean-based canonical [7]	0.61	0.673	0.796	0.816
Skeleton-based method [16]	0.74	0.682	0.791	0.825
Our Method	0.63	0.687	0.820	0.829

Table 5 Retrieval results for the SHREC'15 non-rigid shape retrieval benchmark [32]

	NN	FT	ST	DCG
Classic MDS	0.969	0.731	0.833	0.922
Fast MDS	0.944	0.649	0.766	0.884
Least-squares MDS	0.992	0.863	0.938	0.969
Non-metric MDS	0.991	0.853	0.929	0.965
GPS	0.749	0.453	0.582	0.745
Euclidean-based method [7]	0.978	0.793	0.884	0.943
skeleton-based method [16]	0.986	0.844	0.933	0.964
Our method	0.990	0.810	0.910	0.956
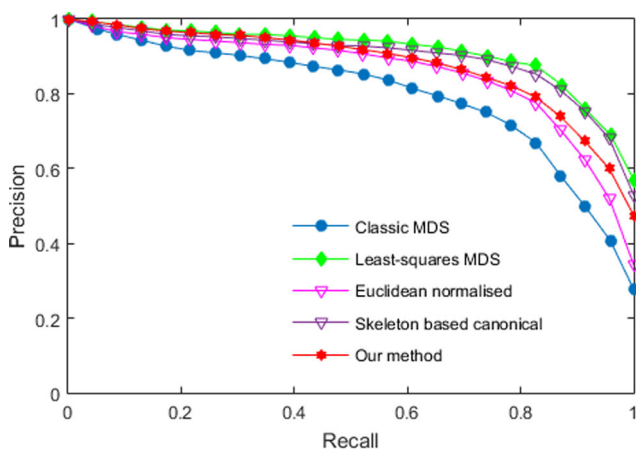
Fig. 9 Precision–recall curves for best methods tested on the SHREC'15 non-rigid benchmark [32] and our method

To sum up, our method is much faster and has lower computational complexity compared to geodesic based methods. It used intrinsic distance based on the Laplace Beltrami operator and provided better results compared to the GPS method. While resulting in only a small difference in performance compared to Euclidean-based method and the skeleton-based method. Moreover, our method is parameter-free and robust to topological errors.

6 Conclusion

In this paper, we have proposed a novel method to construct canonical forms of 3D models based on local MDS method dedicated to non-rigid shape retrieval. We have presented a new idea to divide the problem of 3D canonical form embedding into sub-problems. These sub-problems are solved by adding a spatial constraint between each pairs of them. We have taken advantage of the good properties of the biharmonic distance to add relationship between sub-problems. In addition, we have proposed an automated setting of the weight values in the stress function, in accordance with the values of the dissimilarity matrix and the commute-time weight. Our method does not require all pairs of geodesic distances to be calculated, and then has lower computational complexity than geodesics-based methods. Experiments demonstrated the efficiency of the proposed method to construct invariant 3D canonical forms for 3D non-rigid shape retrieval and achieving, in addition, good retrieval performance in recent 3D non-rigid shapes benchmark.

References

1. Mohamed HH, Belaid S (2015) Algorithm BOSS (bag-of-salient local spectrums) for non-rigid and partial 3D object retrieval. Neurocomputing 168:790–798
2. Pickup D et al (2015) SHREC'15 Track: canonical forms for non-rigid 3d shape retrieval. In: Eurographics Workshop on 3D Object Retrieval, EG 3DOR. https://doi.org/10.2312/3DOR.20151063
3. Mohamed W, Hamza AB (2016) Deformable 3d shape retrieval using a spectral geometric descriptor. Appl Intell 45.2:213–229
4. Pickup D et al (2016) Shape retrieval of non-rigid 3d human models. Int J Comput Vis 120.2:169–193
5. Elad A, Kimmel R (2003) On bending invariant signatures for surface. IEEE Trans Pattern Anal Mach Intell 25(10):1285–1295
6. Lian Z, Godil A, Xiao J (2013) Feature-preserved 3d canonical form. Int J Comput Vis 102:221–238
7. Pickup D, Sun X, Rosin PL, Martin RR (2015) Euclidean-distance-based canonical forms for non-rigid 3D shape retrieval. Pattern Recogn 48(8):2500–2512
8. Bustos B et al (2014) Coulomb shapes: using electrostatic forces for deformation-invariant shape representation. In: Proceedings of the 7th eurographics workshop on 3D Object Retrieval, pp 9–15

9. Mohamed HH, Belaid S, Naanaa W (2017) Local features-based 3d canonical form. In: Proceedings of the 6th international workshop on representations, analysis and recognition of shape and motion from imaging data, Tunisia 2016, appeared also in springer communications in computer and information science series, CCIS 684, pp 1–12. https://doi.org/10.1007/978-3-319-60654-51

10. Borg I, Groenen P (1997) Modern multidimensional scaling-theory and applications. Springer, Berlin

11. Faloutsos C, Lin KD (1995) A fast algorithm for indexing, data mining and visualisation of traditional and multimedia datasets. In: Proceedings of the ACM SIGMOD, pp 163–174

12. Aflalo Y, Kimmel R (2013) Spectral multidimensional scaling. Proc Natl Acad Sci 110(45):18052–18057

13. Shamai G, Zibulevsky M, Kimmel R (2015) Accelerating the computation of canonical forms for 3D nonrigid objects using multidimensional scaling. In: Proceedings of the 2015 eurographics workshop on 3d object retrieval. Eurographics association

14. Xu C, Wang TY, Liu YJ, Liu L, He Y (2015) Fast wavefront propagation (FWP) for computing exact geodesic distances on meshes. IEEE Trans Vis Comput Graph 21(7):822–834

15. Ying X, Xin S-Q (2014) He, y parallel Chen-Han (PCH) algorithm for discrete geodesics. ACM Trans Graph (TOG) 33(1):9

16. Pickup D et al (2016) Skeleton-based canonical forms for non-rigid 3D shape retrieval. Computational Visual Media 2.3:231–243

17. Rustamov RM (2007) Laplace-beltrami eigenfunctions for deformation invariant shape representation. In: Proceedings of the fifth eurographics symposium on geometry processing. Eurographics association

18. Kimmel R, Sethian JA (1998) Computing geodesic paths on manifolds. Proc Natl Acad Sci 95:8431–8435

19. Coifman RR et al (2005) Geometric diffusions as a tool for harmonic analysis and structure definition of data: diffusion maps. Proc Natl Acad Sci U S A 102.21:7426–7431

20. Fouss F, Pirotte A, Renders J-M, Saerens M (2007) Random-walk computation of similarities between nodes of a graph with application to collaborative recommendation. IEEE Trans Knowl Data Eng 19(3):355–369

21. Lipman Y, Rustamov RM, Funkhouser TA (2010) Biharmonic distance. ACM Trans Graph (TOG) 29(3):27

22. Jones PW, Maggioni M, Schul R (2008) Manifold parametrizations by eigenfunctions of the laplacian and heat kernels. Proc Natl Acad Sci 105(6):1803–1808

23. Qiu H, Hancock ER (2007) Clustering and embedding using commute times. IEEE Trans Pattern Anal Mach Intell 29:11

24. Gębal K, Bærentzen JA, Aanæs H, Larsen R (2009) Shape analysis using the auto diffusion function. Computer Graphics Forum 28(5):405–1413

25. Crane K, Weischedel C, Wardetzky M (2013) Geodesics in heat: a new approach to computing distance based on heat flow. ACM Trans Graph 32(5):152

26. Bronstein AM, Bronstein M, Kimmel R (2008) Numerical geometry of non-rigid shapes. Monographs in computer science. Springer

27. Lloyd SP (1982) Least squares quantization in PCM. IEEE Trans Inf Theory IT-28:129–137

28. Lian Z, Godil A, Sun X, Xiao J (2013) CM-BOF: visual similarity-based 3d shape retrieval using clock matching and bag-of-features. Mach Vis Appl 24.8:1685–1704

29. Siddiqi K et al (2008) Retrieving articulated 3-d models using medial surfaces. Mach Vis Appl 19.4:261–275

30. Lian Z, Godil A, Bustos B, Daoudi M, Hermans J, Kawamura S, Kurita Y, Lavoué G, Nguyen HV, Ohbuchi R, Ohkita Y, Ohishi Y, Porikli F, Reuter M, Sipiran I, Smeets D, Suetens P, Tabia H, Vandermeulen D (2011) SHREC'11 track: shape retrieval on non-rigid 3D watertight meshes. In: Proceedings of the 4th eurographics conference on 3d object retrieval, pp 79–88

31. Cheng Z, Lian Z, Aono M, Hamza AB, Bronstein A, Bronstein M, Bu S, Castellani U, Cheng S, Garro V, Giachetti A, Godil A, Han J, Johan H, Lai L, Li B, Li C, Li H, Litman R, Liu X, Liu Z, Lu Y, Tatsuma A, Ye J (2014) Shape retrieval of non-rigid 3D human models. In: Proceedings of the 7th eurographics workshop on 3d object retrieval, pp 101–110

32. Lian Z, Zhang J, Choi S, ElNaghy H, El-Sana J, Furuya T, Giachetti A, Guler RA, Lai L, Li C, Li H, Limberger FA, Martin R, Nakanishi RU, Neto AP, Nonato LG, Ohbuchi R, Pevzner K, Pickup D, Rosin P, Sharf A, Sun L, Sun X, Tari S, Unal G, Wilson RC (2015) Non-rigid 3d shape retrieval. In: Proceedings of the 2015 eurographics workshop on 3d object retrieval, pp 107–120

Hela Haj Mohamed received his Master degree in science and technology from Faculty of science Monastir, University of Monastir-Tunisia in 2013. She joined Modeling of Automated Reasoning Systems (Mars) research lab as a PhD researcher. His research interests include 3D shape analysis and object recognition.

Samir Belaid received his engineering degree in Electronic from National Engineering School of Monastir, Tunisia in 1993 and the PhD degree in Image Processing from Rouen University-France in 1998. Samir Belaid is an associate Professor in the Computer Science Department of the Faculty of science of Monastir-Tunisia. His current research interests include issues related to Computer Vision.

Wady Naanaa has received his PhD degree from the University of Lyon I in 1996. Currently, Wady Naanaa is a Professor of Computer Science at the University of Tunis El Manar (Tunisia). His research activities concern mainly constraint satisfaction and optimization problems.

Lotfi Ben Romdhane holds a Ph.D. degree from the University of Sherbrooke, QC/Canada, and an engineering degree from ENSI/Tunisia; both in computer science. He is currently a Professor in computer science at ISIT'COM, University of Sousse, Tunisia and heads MARS (Modeling of Automated Reasoning Systems) Research Lab. His areas of expertise span the general area of Data Science and include reasoning, distributed computing, knowledge discovery, and data mining. He has published more than 60 papers in these topics in international conferences and journals.